A generalized regularized phase tracker for demodulation of a single fringe pattern

Kai, Li; Qian, Kemao

2012

Kai, L., & Qian K. (2012). A generalized regularized phase tracker for demodulation of a single fringe pattern. Optics Express, 20(11), 12579-12592.

https://hdl.handle.net/10356/95217

https://doi.org/10.1364/OE.20.012579

A generalized regularized phase tracker for demodulation of a single fringe pattern

Li Kai[1] and Qian Kemao[2,*]

[1]*Department of Mechanics, Shanghai University, Shanghai 200444, China*
[2]*School of Computer Engineering, Nanyang Technological University, Singapore 639798, Singapore*
[*]*mkmqian@ntu.edu.sg*

Abstract: The regularized phase tracker (RPT) is one of the most powerful approaches for demodulation of a single fringe pattern. However, two disadvantages limit the applications of the RPT in practice. One is the necessity of a normalized fringe pattern as input and the other is the sensitivity to critical points. To overcome these two disadvantages, a generalized regularized phase tracker (GRPT) is presented. The GRPT is characterized by two novel improvements. First, a general local fringe model that includes a linear background, a linear modulation and a quadratic phase is adopted in the proposed enhanced cost function. Second, the number of iterations in the optimization process is proposed as a comprehensive measure of fringe quality and used to guide the demodulation path. With these two improvements, the GRPT can directly demodulate a single fringe pattern without any pre-processing and post-processing and successfully get rid of the problem of the sensitivity to critical points. Simulation and experimental results are presented to demonstrate the effectiveness and robustness of the GRPT.

OCIS codes: (100.5070) Phase retrieval; (100.2650) Fringe analysis; (120.5050) Phase measurement; (120.3940) Metrology.

References and links

1. G. Cloud, *Optical Methods of Engineering Analysis* (Cambridge U. Press, Cambridge, UK, 1995).
2. D. Malacara, M. Servin, and Z. Malacara, *Interferogram Analysis for Optical Testing, 2nd ed.* (Marcel Deker, 2003).
3. J. H. Bruning, D. R. Herriott, J. E. Gallagher, D. P. Rosenfeld, A. D. White, and D. J. Brangaccio, "Digital wavefront measuring interferometer for testing optical surfaces and lenses," Appl. Opt. **13**(11), 2693–2703 (1974).
4. K. Creath, "Temporal phase measurement methods," in *Interferogram Analysis: Digital Fringe Pattern Measurement Technique*, D. W. Robinson and G. T. Reid, eds. (Institute of Physics, 1993), Chap. 4, pp. 94–140.
5. M. Takeda, H. Ina, and S. Kobayashi, "Fourier-transform method of fringe pattern analysis for computer-based topography and interferometry," J. Opt. Soc. Am. **72**(1), 156–160 (1982).
6. T. Kreis, "Digital holographic interference-phase measurement using the Fourier-transform method," J. Opt. Soc. Am. A **3**(6), 847–855 (1986).
7. J. L. Marroquin, M. Servin, and R. Rodriguez-Vera, "Adaptive quadrature filters and the recovery of phase from fringe pattern images," J. Opt. Soc. Am. A **14**(8), 1742–1753 (1997).
8. J. L. Marroquin, R. Rodriguez-Vera, and M. Servin, "Local phase from local orientation by solution of a sequence of linear systems," J. Opt. Soc. Am. A **15**(6), 1536–1544 (1998).
9. K. G. Larkin, D. J. Bone, and M. A. Oldfield, "Natural demodulation of two-dimensional fringe patterns. I. general background of the spiral phase quadrature transform," J. Opt. Soc. Am. A **18**(8), 1862–1870 (2001).
10. M. Servin, J. A. Quiroga, and J. L. Marroquin, "General n-dimensional quadrature transform and its application to interferogram demodulation," J. Opt. Soc. Am. A **20**(5), 925–934 (2003).
11. E. Robin and V. Valle, "Phase Demodulation from a Single Fringe Pattern Based on a Correlation Technique," Appl. Opt. **43**(22), 4355–4361 (2004).
12. E. Robin, V. Valle, and F. Brémand, "Phase demodulation method from a single fringe pattern based on correlation with a polynomial form," Appl. Opt. **44**(34), 7261–7269 (2005).
13. M. Rivera, "Robust phase demodulation of interferograms with open or closed fringes," J. Opt. Soc. Am. A **22**(6), 1170–1175 (2005).
14. J. C. Estrada, M. Servin, and J. L. Marroquín, "Local adaptable quadrature filters to demodulate single fringe patterns with closed fringes," Opt. Express **15**(5), 2288–2298 (2007), http://www. opticsinfobase.org/ oe/abstract. cfm?URI = oe-15–5-2288.

#165020 - $15.00 USD Received 19 Mar 2012; revised 6 May 2012; accepted 8 May 2012; published 18 May 2012

15. Q. Kemao and S. Hock Soon, "Sequential demodulation of a single fringe pattern guided by local frequencies," Opt. Lett. **32**(2), 127–129 (2007).
16. O. Dalmau-Cedeño, M. Rivera, and R. Legarda-Saenz, "Fast phase recovery from a single close-fringe pattern," J. Opt. Soc. Am. A **25**(6), 1361–1370 (2008).
17. M. Servin, J. L. Marroquin, and F. J. Cuevas, "Demodulation of a single interferogram by use of a two-dimensional regularized phase-tracking technique," Appl. Opt. **36**(19), 4540–4548 (1997).
18. R. Legarda-Sáenz, W. Osten, and W. Jüptner, "Improvement of the Regularized Phase Tracking Technique for the Processing of Nonnormalized Fringe Patterns," Appl. Opt. **41**(26), 5519–5526 (2002).
19. R. Legarda-Saenz and M. Rivera, "Fast half-quadratic regularized phase tracking for nonnormalized fringe patterns," J. Opt. Soc. Am. A **23**(11), 2724–2731 (2006).
20. M. Servin, J. L. Marroquin, and F. J. Cuevas, "Fringe-follower regularized phase tracker for demodulation of closed-fringe interferograms," J. Opt. Soc. Am. A **18**(3), 689–695 (2001).
21. H. Wang and Q. Kemao, "Frequency guided methods for demodulation of a single fringe pattern," Opt. Express **17**(17), 15118–15127 (2009), http://www.opticsinfobase.org/abstract.cfm?URI=oe-17-17-15118.
22. C. Tian, Y. Y. Yang, D. Liu, Y. J. Luo, and Y. M. Zhuo, "Demodulation of a single complex fringe interferogram with a path-independent regularized phase-tracking technique," Appl. Opt. **49**(2), 170–179 (2010).
23. H. Wang, K. Li, and Q. Kemao, "Frequency guided methods for demodulation of a single fringe pattern with quadratic phase matching," Opt. Lasers Eng. **49**(4), 564–569 (2011).
24. J. Nocedal and S. J. Wright, *Numerical Optimization* (Springer, 1999).
25. J. A. Quiroga, J. Antonio Gómez-Pedrero, and Á. García-Botella, "Algorithm for fringe pattern normalization," Opt. Commun. **197**(1-3), 43–51 (2001).
26. J. Antonio Quiroga and M. Servin, "Isotropic n-dimensional fringe pattern normalization," Opt. Commun. **224**(4-6), 221–227 (2003).
27. J. A. Guerrero, J. L. Marroquin, M. Rivera, and J. A. Quiroga, "Adaptive monogenic filtering and normalization of ESPI fringe patterns," Opt. Lett. **30**(22), 3018–3020 (2005).
28. N. A. Ochoa and A. A. Silva-Moreno, "Normalization and noise-reduction algorithm for fringe patterns," Opt. Commun. **270**(2), 161–168 (2007).
29. M. B. Bernini, A. Federico, and G. H. Kaufmann, "Normalization of fringe patterns using the bidimensional empirical mode decomposition and the Hilbert transform," Appl. Opt. **48**(36), 6862–6869 (2009).
30. Q. Kemao, "Windowed Fourier transform for fringe pattern analysis," Appl. Opt. **43**(13), 2695–2702 (2004).
31. Q. Kemao, "Two-dimensional windowed Fourier transform for fringe pattern analysis: Principles, applications and implementations," Opt. Lasers Eng. **45**(2), 304–317 (2007).
32. W. H. Press, S. A. Teukolsky, W. T. Vetterling, and B. P. Flannery, *Numerical Recipes in C,* 2nd ed. (Cambridge University, Cambridge, England, 1999).
33. D. C. Ghiglia and M. D. Pritt, *Two-Dimensional Phase Unwrapping: Theory, Algorithms, and Software* (John Wiley & Sons, Inc, 1998).
34. M. Zhao, L. Huang, Q. Zhang, X. Y. Su, A. Asundi, and Q. Kemao, "Quality-guided phase unwrapping technique: comparison of quality maps and guiding strategies," Appl. Opt. **50**(33), 6214–6224 (2011).
35. M. Bertero and P. Boccacci, *Introduction to Inverse Problems in Imaging* (Institute of Physics, London, 1998), Chap. 5.

1. Introduction

Most optical measurement techniques provide their measurement results in the form of fringe patterns. Depending on the applications, various physical quantities such as displacement, temperature, surface profile and refractive index, can be encoded in fringe patterns [1]. A fringe pattern can be typically represented by the following mathematical expression:

$$f(x,y) = a(x,y) + b(x,y)\cos\left[\varphi(x,y)\right] + n(x,y), \tag{1}$$

where (x,y) is the pixel coordinate; $f(x,y)$ denotes the recorded intensity of the fringe pattern; $a(x,y)$ is the background; $b(x,y)$ is the modulation; $\varphi(x,y)$ is the phase term related to the physical quantity being measured; $n(x,y)$ is the noise term. The common objective of fringe pattern analysis is to recover the phase $\varphi(x,y)$ from the intensity $f(x,y)$.

A number of well-known techniques have been developed for phase demodulation from fringe patterns [2]. Among them, phase shifting technique is the best choice provided that the experiment condition permits one to acquire several phase-shifted fringe patterns [3, 4]. Fourier transform is another widely used method when a carrier frequency can be introduced to the fringe pattern [5, 6]. However, in some experiments such as the transient mechanical processes, it is difficult to acquire multiple phase-shifted fringe patterns or introduce a carrier

#165020 - $15.00 USD Received 19 Mar 2012; revised 6 May 2012; accepted 8 May 2012; published 18 May 2012

frequency to the fringe pattern. In such situations, demodulation of a single fringe pattern becomes important.

Various methods have been developed for phase demodulation from a single fringe pattern [7–23], such as the adaptive quadrature filters, the spiral phase quadrature transform, the correlation technique and the regularized phase tracker (RPT). The RPT [17] is one of the most powerful approaches and has been well recognized. However, the RPT has two disadvantages: the necessity of a normalized fringe pattern as input and the sensitivity to critical points. To overcome the first disadvantage, Ricardo et al. proposed an improved RPT [18] by including the modulation into the cost function of the RPT, so that a nonnormalized fringe pattern can be demodulated. This work was further improved for better optimization results by introducing a rough estimate of the modulation and the linearization of the local fringe model [19]. To overcome the second disadvantage, Servin et al. proposed the fringe follower regularized phase tracker (FFRPT) [20], which used the fringe intensity to guide the demodulation path in order to isolate the critical points. Wang et al. proposed a more robust scanning strategy called frequency guided regularized phase tracker (FGRPT) [21], which used the local frequency to guide the demodulation path. Tian et al. proposed a path independent regularized phase tracker (PIRPT) [22], where a quadratic phase is adopted to replace the linear phase model in the original RPT. Because the quadratic phase can match the local fringe data more precisely, the PIRPT is less sensitive to the critical points and is able to achieve a higher accuracy for phase. Recently, Wang et al. proposed a quadratic phase matching and frequency guided regularized phase tracker (QFGRPT), which is the combination of the advantages of FGRPT and PIRPT and indeed was demonstrated to be more robust and accurate [23].

Nevertheless, there still lacks a technique that overcomes both disadvantages. In this paper, a generalized regularized phase tracker (GRPT) is presented to achieve this goal, which is made possible by including two novel improvements. First, a general local fringe model that includes a linear background, a linear modulation and a quadratic phase is adopted in the cost function, and twelve parameters are optimized simultaneously. The optimization will be seen successful by selecting proper initial values. Second, the number of iterations in the optimization process is used to guide the demodulation path, which reflects the quality of the fringe pattern and automatically postpone the processing of critical points, noisy areas, image borders, and even phase discontinuities. Based on these two improvements, the GRPT can directly and successfully demodulate a single fringe pattern without any pre-processing and post-processing. Simulation and experimental results are presented to demonstrate the effectiveness and robustness of the GRPT.

The rest of the paper is organized as follows. The RPT will be briefly reviewed in Sec. 2. The proposed GRPT will then be presented in Sec. 3. Results and discussions will be given in Sec. 4. The problem of phase demodulation from a single fringe pattern with phase discontinuities is discussed in Sec. 5. A conclusion will be drawn in Sec. 6.

2. Regularized phase tracker

The basic idea of the RPT [17] is that the fringe pattern is considered as locally monochromatic, that is, the local fringe can be modeled as a cosinusoidal function of linear phase. The cost function to be minimized for parameter estimation is defined as [17]

$$U(x,y)=\sum_{(\varepsilon,\eta)\in N_{x,y}}\left\{\left[f_n(\varepsilon,\eta)-f_e(x,y;\varepsilon,\eta)\right]^2+\lambda\left[\varphi_0(\varepsilon,\eta)-\varphi_e(x,y;\varepsilon,\eta)\right]^2 m(\varepsilon,\eta)\right\}, \quad (2)$$

with

$$f_n(\varepsilon,\eta)\approx\cos\left[\varphi(\varepsilon,\eta)\right], \quad (3)$$

$$f_e(x,y;\varepsilon,\eta)=\cos\left[\varphi_e(x,y;\varepsilon,\eta)\right], \quad (4)$$

#165020 - $15.00 USD Received 19 Mar 2012; revised 6 May 2012; accepted 8 May 2012; published 18 May 2012

$$\varphi_e(x,y;\varepsilon,\eta)=\varphi_0(x,y)+\omega_x(x,y)(\varepsilon-x)+\omega_y(x,y)(\eta-y), \tag{5}$$

where $N_{x,y}$ is a neighborhood region around (x,y) with coordinates (ε,η); $f_n(\varepsilon,\eta)$ is the normalized fringe pattern obtained by normalizing a fringe pattern in Eq. (1); $f_e(x,y;\varepsilon,\eta)$ is the local fringe model that gives the intensity distribution in $N_{x,y}$; $\varphi_e(x,y;\varepsilon,\eta)$ indicates the assumed phase distribution in $N_{x,y}$; $\varphi_0(x,y)$ is the phase estimation; $\omega_x(x,y)$ and $\omega_y(x,y)$ are the first order phase derivatives in the x and y directions, respectively; they are also called as the local frequency estimations in the x and y directions, respectively; $m(\varepsilon,\eta)$ is an indicator that equals one if the pixel (ε,η) has already been demodulated and equals zero otherwise; λ is a regularizing parameter that controls the smoothness of the phase estimation $\varphi_0(x,y)$. The first term in Eq. (2), also called a fidelity term, attempts to keep the local fringe model $f_e(x,y;\varepsilon,\eta)$ close to the normalized fringe pattern $f_n(\varepsilon,\eta)$ in a least squares sense within the neighborhood $N_{x,y}$. The second term, also called a regularization term, enforces the phase estimation $\varphi_0(x,y)$ to be smooth to the already estimated phases marked by $m(\varepsilon,\eta)$. By minimizing the cost function in Eq. (2) on a pixel-by-pixel basis with respect to three parameters $\varphi_0(x,y)$, $\omega_x(x,y)$ and $\omega_y(x,y)$, the given fringe pattern can be demodulated. A gradient descent method is adopted for optimization in [17, 20], while other iterative optimization methods can also be used [24]. The resultant phase estimation is continuous and no further unwrapping process is required.

Two disadvantages of the RPT mentioned in Sec. 1 can be more clearly observed from the RPT model in Eqs. (2)-(5). First, a normalized fringe pattern $f_n(\varepsilon,\eta)$ is used as input in Eq. (2), but the normalization is a difficult task [25–29]. Second, from the fidelity term in Eq. (2), if $\left[\varphi_0(x,y),\omega_x(x,y),\omega_y(x,y)\right]$ is a solution, so is $\left[-\varphi_0(x,y),-\omega_x(x,y),-\omega_y(x,y)\right]$, which results in the phase ambiguity problem. In the RPT, this problem can be solved by two facts: (i) the estimation in a neighboring pixel is used as the initial value of the current pixel, which implicitly enforces the continuity of the parameters; and (ii) the regularization term explicitly enforces the continuity of phase estimation. However, neither fact is effective when the current pixel is around critical points (maxima, minima and saddles) where all parameters are close to zero and can result in spurious phase signs. Once one pixel has the wrong sign, the error will propagate to subsequently processed pixels. Improvements to overcome the first or second disadvantages have been discussed in Sec. 1. An algorithm that is able to overcome both disadvantages is lacking but highly desired.

3. Generalized regularized phase tracker

In this section, we propose a generalized regularized phase tracker (GRPT) that can simultaneously overcome the two disadvantages of the RPT and therefore, the GRPT can directly demodulate a fringe pattern without any pre-processing and post-processing. Two novel improvements of the GRPT are detailed in Secs. 3.1 and 3.2, respectively. The overall algorithm is outlined in Sec. 3.3.

3.1 An enhanced cost function for the GRPT

In order to directly demodulate a fringe pattern without normalization, we model $a(x,y)$ and $b(x,y)$ as locally linear, and $\varphi(x,y)$ as locally quadratic. The local fringe in $N_{x,y}$ is thus expressed as follows,

#165020 - $15.00 USD Received 19 Mar 2012; revised 6 May 2012; accepted 8 May 2012; published 18 May 2012

$$f_e(x,y;\varepsilon,\eta)=a_e(x,y;\varepsilon,\eta)+b_e(x,y;\varepsilon,\eta)\cos\left[\varphi_e(x,y;\varepsilon,\eta)\right], \tag{6}$$

$$a_e(x,y;\varepsilon,\eta)=a_0(x,y)+a_x(x,y)(\varepsilon-x)+a_y(x,y)(\eta-y), \tag{7}$$

$$b_e(x,y;\varepsilon,\eta)=b_0(x,y)+b_x(x,y)(\varepsilon-x)+b_y(x,y)(\eta-y), \tag{8}$$

$$\begin{aligned}\varphi_e(x,y;\varepsilon,\eta)=&\varphi_0(x,y)+\omega_x(x,y)(\varepsilon-x)+\omega_y(x,y)(\eta-y)+\frac{c_{xx}(x,y)}{2}(\varepsilon-x)^2\\&+\frac{c_{yy}(x,y)}{2}(\eta-y)^2+c_{xy}(x,y)(\varepsilon-x)(\eta-y),\end{aligned} \tag{9}$$

where $f_e(x,y;\varepsilon,\eta)$ denotes the general local fringe model in $N_{x,y}$; $a_e(x,y;\varepsilon,\eta)$ is the local background model in $N_{x,y}$; $a_0(x,y)$ is the background estimation; $a_x(x,y)$ and $a_y(x,y)$ are the first order derivatives of the background in the x and y directions, respectively; similarly, $b_e(x,y;\varepsilon,\eta)$ is the local modulation model in $N_{x,y}$; $b_0(x,y)$ is the modulation estimation; $b_x(x,y)$ and $b_y(x,y)$ are the first order derivatives of modulation in the x and y directions, respectively; $\varphi_e(x,y;\varepsilon,\eta)$ is the local phase model in $N_{x,y}$; $\varphi_0(x,y)$ is the phase estimation; $\omega_x(x,y)$, $\omega_y(x,y)$, $c_{xx}(x,y)$, $c_{yy}(x,y)$ and $c_{xy}(x,y)$ are the first and second order phase derivatives.

With this general fringe model, the cost function in Eq. (2) is adapted and enhanced as follows,

$$U(x,y)=\sum_{(\varepsilon,\eta)\in N_{x,y}}\left(w(x,y;\varepsilon,\eta)\left\{\left[f(\varepsilon,\eta)-f_e(x,y;\varepsilon,\eta)\right]^2+\lambda\left[\varphi_0(\varepsilon,\eta)-\varphi_e(x,y;\varepsilon,\eta)\right]^2 m(\varepsilon,\eta)\right\}\right) \tag{10}$$

where $w(x,y;\varepsilon,\eta)$ is a Gaussian window with a standard deviation σ,

$$w(x,y;\varepsilon,\eta)=\exp\left[-\frac{(x-\varepsilon)^2+(y-\eta)^2}{2\sigma^2}\right]. \tag{11}$$

In this paper, the neighborhood $N_{x,y}$ is a square region of $W\times W$ pixels and the standard deviation σ of the Gaussian window is defined as $\sigma=W/4$. Compared with the cost function of the RPT in Eq. (2), the enhanced model is more general and elegant by estimating background, modulation and phase simultaneously. This cost is that there are twelve parameters, $a_0(x,y)$, $a_x(x,y)$, $a_y(x,y)$, $b_0(x,y)$, $b_x(x,y)$, $b_y(x,y)$, $\varphi_0(x,y)$, $\omega_x(x,y)$, $\omega_y(x,y)$, $c_{xx}(x,y)$, $c_{yy}(x,y)$, and $c_{xy}(x,y)$, to be optimized simultaneously. This turns out to be achievable by setting initial values properly [23]. For the seed pixel (x_0,y_0), i.e., the first pixel to be demodulated, the initial values are set as follows: $a_0(x_0,y_0)=mean\left[f(x,y)\right]$, i.e., the mean of the fringe pattern in the neighborhood N_{x_0,y_0}; $a_x(x_0,y_0)=a_y(x_0,y_0)=0$, $b_0(x_0,y_0)$, $\varphi_0(x_0,y_0)$, $\omega_x(x_0,y_0)$ and $\omega_y(x_0,y_0)$ are estimated by the windowed Fourier ridges method [30, 31]; $b_x(x_0,y_0)=b_y(x_0,y_0)=0$;

#165020 - $15.00 USD Received 19 Mar 2012; revised 6 May 2012; accepted 8 May 2012; published 18 May 2012

$c_{xx}(x_0, y_0) = c_{yy}(x_0, y_0) = c_{xy}(x_0, y_0) = 0$. For a subsequent pixel (x, y), the initial values are set according to its already demodulated adjacent pixel (x_s, y_s) as follows,

$$
\begin{aligned}
a_0(x,y) &= a_0(x_s,y_s) + a_x(x_s,y_s)(x-x_s) + a_y(x_s,y_s)(y-y_s)\\
a_x(x,y) &= a_x(x_s,y_s)\\
a_y(x,y) &= a_y(x_s,y_s)\\
b_0(x,y) &= b_0(x_s,y_s) + b_x(x_s,y_s)(x-x_s) + b_y(x_s,y_s)(y-y_s)\\
b_x(x,y) &= b_x(x_s,y_s)\\
b_y(x,y) &= b_y(x_s,y_s)\\
\varphi_0(x,y) &= \varphi_0(x_s,y_s) + \omega_x(x_s,y_s)(x-x_s) + \omega_y(x_s,y_s)(y-y_s)\\
&\quad + c_{xx}(x_s,y_s)(x-x_s)^2/2 + c_{yy}(x_s,y_s)(y-y_s)^2/2\\
&\quad + c_{xy}(x_s,y_s)(x-x_s)(y-y_s)\\
\omega_x(x,y) &= \omega_x(x_s,y_s) + c_{xx}(x_s,y_s)(x-x_s) + c_{xy}(x_s,y_s)(y-y_s)\\
\omega_y(x,y) &= \omega_y(x_s,y_s) + c_{yy}(x_s,y_s)(y-y_s) + c_{xy}(x_s,y_s)(x-x_s)\\
c_{xx}(x,y) &= c_{xx}(x_s,y_s)\\
c_{yy}(x,y) &= c_{yy}(x_s,y_s)\\
c_{xy}(x,y) &= c_{xy}(x_s,y_s).
\end{aligned}
\tag{12}
$$

Two optimization methods, Levenberg-Marquardt (LM) method [32] and Broyden-Fletcher-Goldfarb-Shanno (BFGS) method [24], have been tested and both are capable of our demodulation. The LM method is chosen in this paper for its better performance. To implement the LM method, the condition of convergence is set as $|\nabla U(x,y)| < \zeta$, where $|\nabla U(x,y)|$ denotes the norm of the gradient of the cost function in Eq. (10) and ζ is a small positive number. The successful demodulation by optimization will be demonstrated in Sec. 4 through various examples.

3.2 An effective scanning strategy of the GRPT

As mentioned in Sec. 2, critical points often cause the problem of spurious phase signs and then result in errors propagation. The most effective way to solve this problem is the quality guided scanning strategy [33, 34] by assigning low quality to critical points. Two scanning strategies, the fringe follower scanning strategy [20] and the frequency guided scanning strategy [21], have been used for the RPT. The latter was demonstrated to be more robust since it can distinguish the critical points more effectively.

Naturally the success of the frequency guidance relies on reliable estimation of local frequencies. It can be easily achieved in [21] where the fringe patterns have been successfully denoised and normalized before frequency estimation, but is more difficult in the proposed enhanced model in Eq. (10) where the fringe patterns to be demodulated are generally noisy and nonnomalized. The accuracy reduction of frequency estimation may accumulate to a demodulation failure. To obtain more reliable frequency estimation against noise, a larger window is often needed which can reduce the phase estimation accuracy.

A new scanning strategy is proposed in this paper, which uses the number of iterations (NI) for scanning path guidance. The NI refers to number of iterations needed to reach the predetermined convergence condition when an iterative optimization algorithm is performed to minimize the cost function given in Eq. (10). We find that the NI is large at the critical

#165020 - $15.00 USD Received 19 Mar 2012; revised 6 May 2012; accepted 8 May 2012; published 18 May 2012

points and their neighborhood pixels. In addition, the NI is also large in the regions with heavy noise, near image borders, or near phase discontinuities. Thus NI is discovered to be a comprehensive measure of overall fringe quality. This discovery inspires us to propose a new scanning strategy using the NI as the quality map to guide the demodulation path. In the NI guided scanning strategy, the pixels with smaller NIs are processed earlier than those with larger NIs, which not only postpones the processing of critical points, noisy pixels and pixels near image borders, but also recognizes phase discontinuities. Surprisingly good results will be reported in Secs. 4 and 5.

3.3 The proposed GRPT

Based on the enhanced cost function in Sec. 3.1 and the NI guided scanning strategy in Sec. 3.2, the proposed GRPT is the NI guided minimization of the enhanced cost function given in Eq. (10). The GRPT algorithm is outlined as follows.

Step 1: Select a pixel with high signal-to-noise ratio, high local frequency and away from image borders as the seed pixel (x_0, y_0);

Step 2: Demodulate the seed pixel by minimizing the cost function in Eq. (10); push the seed pixel into a demodulation register. Only one register is needed for the GRPT;

Step 3: Select the pixel (x_s, y_s) with the lowest NI in the demodulation register; demodulate its unprocessed adjacent pixels by minimizing the cost function in Eq. (10); remove the selected pixel from the register;

Step 4: Push the processed pixels into the register and sort the pixels according to their NIs;

Step 5: Repeat step 3 and step 4 until the register is empty.

It should be pointed out that the LM algorithm used to minimize the cost function Eq. (10) is indeed a local optimization algorithm and its success mainly depends on two factors. One is the initial values and the other is the solution space of the cost function Eq. (10). In the GRPT, these two factors are elegantly solved. For the seed pixel, since a high signal-to-noise ratio can be selected and the robust WFR method is used, its initial values can be accurately estimated. For a subsequent pixel, the initial values can be estimated according to its already demodulated adjacent pixel, as expressed in Eq. (12). Considering the complexity of the solution space of the cost function Eq. (10), the LM algorithm may be failed, especially at these pixels with low signal-to-noise ratio, near image borders and critical points. However, these pixels are automatically postponed for processing in the GRPT since the NI guided scanning strategy is adopted, and consequently the GRPT is able to success.

4. Results and discussions

To verify the effectiveness and robustness of the proposed GRPT, some simulated and experimental fringe patterns are demodulated. All calculations are carried out on a personal Pentium Dual E8400 computer with 3.0GHz main frequency by C + + programming. A 31×31 neighborhood for $N_{x,y}$ is used for all the calculations in this paper. The convergence condition for the LM method in minimizing the cost function of the GRPT is $\left|\nabla U(x,y)\right| < 0.01$ and in addition, a maximum iteration number of 10 is used to stop the iterative calculations for the non-convergence pixels. All retrieved phase results from the GRPT are already unwrapped, which will be rewrapped for displaying purpose.

4.1 Results from a simulated typical fringe pattern and discussions

A typical computer-generated fringe pattern of size 256×256 is shown in Fig. 1(a) with its true phase shown in Fig. 1(b). Figure 1(c) shows the corresponding ideal fringe pattern. It can be seen that the fringe pattern shown in Fig. 1(a) is degraded by speckle noise and has

#165020 - $15.00 USD Received 19 Mar 2012; revised 6 May 2012; accepted 8 May 2012; published 18 May 2012

nonuniform background and modulation. Moreover, the fringe pattern contains a number of critical points. All these factors make the demodulation of Fig. 1(a) difficult. The GRPT with $\lambda = 20$ is used to demodulate Fig. 1(a). Figure 1(d) shows the NI map (the gray level of Fig. 1(d) is proportional to the NI), which is obtained along with the demodulation of Fig. 1(a) by the GRPT. It can be seen that the problematical regions (pixels around the critical points and near the image edges) are successfully and automatically distinguished in the NI map as pixels with large NIs. Figures 1(e)-1(g) are three snapshots showing the sequence of the GRPT demodulation. From these snapshots, it can be seen that the critical points are well avoided and the pixels near the image borders are postponed to the end. Figure 1(h) shows the final phase result obtained by the GRPT, which is satisfactory. The mean absolute errors (MAE) of the result, i.e., the mean value of the absolute difference between the extracted phase distribution in Fig. 1(h) and the true phase distribution in Fig. 1(b), is calculated to be 0.15 rad. The calculation time is about 11min.

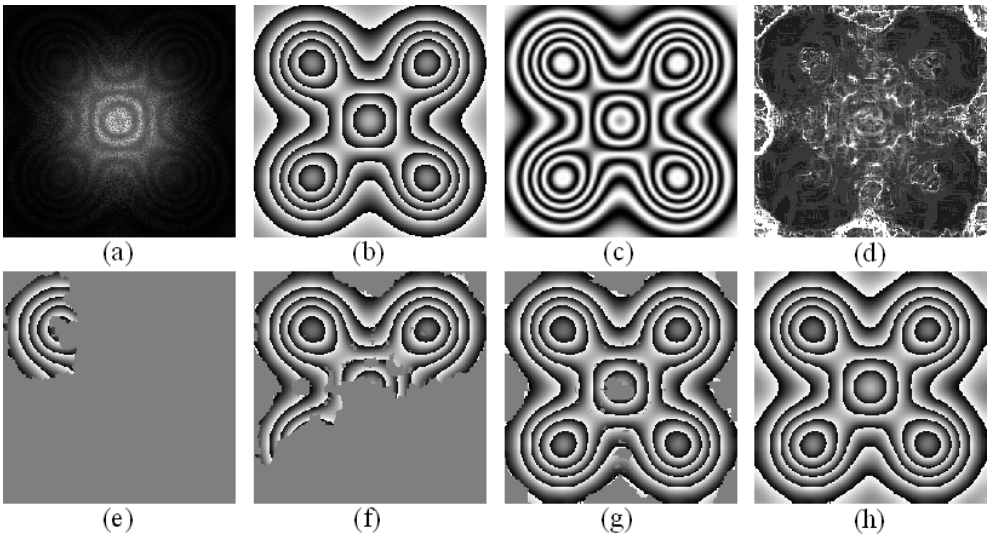

Fig. 1. Demodulation of a computer-generated fringe pattern by the GRPT. (a) computer-generated fringe pattern; (b) the true phase of the fringe pattern; (c) the ideal fringe pattern; (d) the NI map obtained along with the demodulation of (a) by the GRPT; (e)-(g) three snapshots of the estimated phase results obtained by the GRPT; (h) rewrapped phase result obtained by the GRPT.

To further understand the GRPT, influences of its factors and comparison with the FGRPT are investigated below.

(i) Guiding strategy (the NI vs the frequency guidance) The frequency guided scanning strategy is also tested for comparison. Except that NI is replaced by the frequency guidance, all other parameters remain the same. Figures 2(a) and 2(b) show two snapshots of the demodulation. As shown in Fig. 2(b), the demodulation is failed at a certain pixel and the errors then propagated to the following pixels. A possible way is to increases the window size so as to increases the reliability of frequency estimation against the noise. Indeed when the window size is 45×45, the frequency guidance succeeds the demodulation. However usually a larger window will make the assumptions in Eqs. (6)-(9) less reasonable, which leads to a larger phase error. In this example, the MAE using frequency guidance is 0.30 rad, which is two times of that by the NI .

(ii) Window shape (Gaussian vs rectangular) The rectangular window has been traditionally used in the original and improved RPTs. It has a compact shape and fully utilizes the fringe data within the window, which is suitable for the previous

#165020 - $15.00 USD Received 19 Mar 2012; revised 6 May 2012; accepted 8 May 2012; published 18 May 2012

strong assumption of linear phase. In our enhanced model, the assumption of quadratic phase enables us to use a larger window. The Gaussian window is less compact compared with the rectangle window but it is physically more reasonable. Nevertheless, the discrepancy between their performances is small. As an example, Fig. 2(c) shows the demodulation result with a rectangular window, which is also successful but with a higher MAE of 0.21 rad.

(iii) Window size (small vs large) To balance the noise influence and fringe model assumption, a proper window size should be selected. A series of different window size is used to demodulate Fig. 1(a) by the GRPT with $\lambda = 20$. Table 1 shows the MAEs of the obtained results. It can be seen that the demodulation is failed at the window size 21×21 which means the window size is too small to resist the noise. On the other hand, when the window size becomes large, the demodulation accuracy is reduced since the fringe model assumptions in Eqs. (6)-(9) are less reasonable. The window size of 31×31 is found to be the best among the tested window sizes and, according to our experiences, the window size in the range of $25\times 25 \sim 35\times 35$ is suitable for most fringe patterns.

(iv) Regularizing parameter (low vs high) The regularizing parameter λ balances the fidelity term and regularization term. A larger λ emphasizes more on the regularization term. The selection of λ is usually empirical [35]. Two different regularizing parameters, $\lambda = 0$ and $\lambda = 100$, are tested, and the corresponding results are shown in Figs. 2(d) and 2(e), respectively. The demodulation with $\lambda = 0$ is failed at the regions near the image borders as shown in Fig. 2(d). On the other hand, the demodulation with $\lambda = 100$ is successful as shown in Fig. 2(e), but with MAE of 0.21 rad which is larger than that with $\lambda = 20$. According to our experiences, $\lambda = 10 \sim 100$ is suitable for most fringe patterns and therefore is recommended.

(v) Overall performance (the GRPT vs the QFGRPT) Although the QFGRPT [23] needs a normalized fringe pattern as input, it adopts quadratic phase assumption and frequency guidance, and thus is a close relative to the GPRT. It is of interest to compare these two methods. Figure 1(a) is normalized and shown in Fig. 2(f) by performing the Hilbert transform [25] and the windowed Fourier filtering [30, 31]. The QFGRPT is then used to demodulate the normalized fringe pattern. Figure 2(g) shows the frequency map obtained along with the demodulation by the QFGRPT. The demodulation result is shown in Fig. 2(h), with an MAE of 0.32 rad. One major problem causing the higher MAE is that the fringe pattern is slightly distorted when it is normalized, which is unavoidable in most fringe pattern normalization algorithms [25–29].

#165020 - $15.00 USD Received 19 Mar 2012; revised 6 May 2012; accepted 8 May 2012; published 18 May 2012

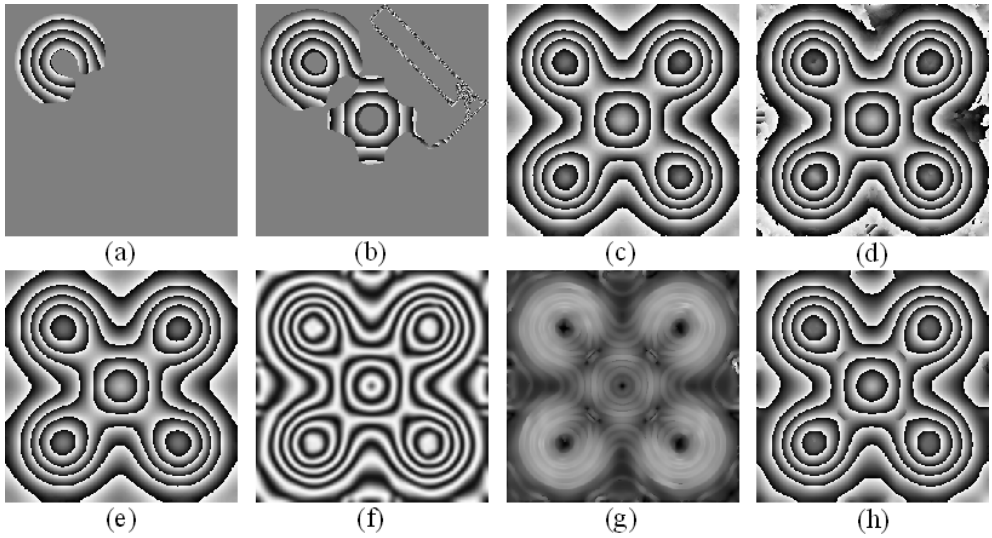

Fig. 2. Some comparative demodulation results of Fig. 1(a). (a)-(b) two snapshots of the estimated phase results obtained by the GRPT using the frequency guided strategy instead of the NI guided strategy; (c) rewrapped phase result obtained by the GRPT using a rectangular window instead of the Gaussian window; (d) rewrapped phase result obtained by the GRPT with the regularizing parameter $\lambda = 0$; (e) rewrapped phase result obtained by the GRPT with the regularizing parameter $\lambda = 100$; (f) normalized fringe pattern from the fringe pattern in Fig. 1(a); (g) the frequency map obtained along with the demodulation of (f) by the QFGRPT [23]; (h) rewrapped phase result obtained by the QFGRPT guided by the frequency map in (g).

Table 1. Demodulation Results

Window Size	21×21	25×25	31×31	35×35	41×41	45×45
Mean absolute error	Failed	0.16	0.15	0.16	0.23	0.25

4.2 Results from more simulated fringe patterns

Another four complex computer-generated fringe patterns are demodulated to show the robustness of the GRPT. The simulated fringe patterns, shown in first column of Fig. 3, have the same size of 200×200. Their true phase distributions are shown in the second column. All these fringe patterns are contaminated by speckle noise and have nonuniform backgrounds and modulations. The parameters are set the same as for Fig. 1. The third column shows the NI maps obtained along with the demodulation of the fringe patterns, which successfully guide the demodulation. The retrieved phase results are shown in the fourth column and their MAEs are 0.13, 0.15, 0.15 and 0.18, respectively. It can be seen that the demodulated phase distributions are satisfactory. The average calculation time for the GRPT to demodulate one of the fringe patterns shown in Fig. 3 is about 6min.

#165020 - $15.00 USD Received 19 Mar 2012; revised 6 May 2012; accepted 8 May 2012; published 18 May 2012

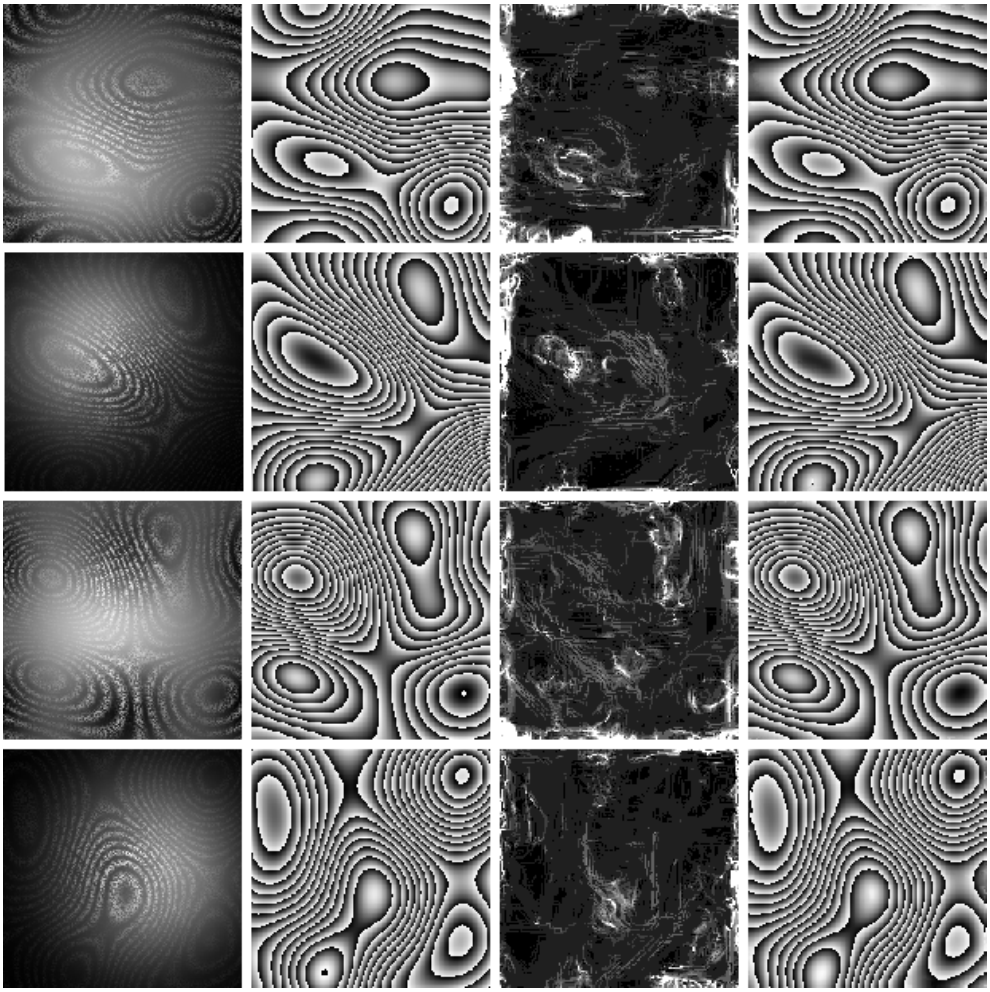

Fig. 3. Four complex computer-generated fringe patterns demodulated by the GRPT. First column shows the four computer-generated fringe patterns; second column shows the true phase distributions of the fringe patterns; third column is the NI maps obtained by the GRPT along with the fringe patterns demodulation; fourth column shows the rewrapped phase results obtained by the GRPT.

4.3 Results from experimental fringe patterns

Finally, two experimental speckle fringe patterns are used for verification. Except for setting $\lambda = 60$, all other parameters remain the same as for Fig. 1. The first example is from speckle shearography with a size of 176×176 and is shown in Fig. 4(a). It has two critical points and is degraded by speckle noise. Figure 4(b) shows the NI map of Fig. 4(a). The problematical regions of the fringe pattern are well distinguished in the NI map. Figures 4(c)-4(f) show four snapshots of the demodulation of Fig. 4(a) by the GRPT. It can be seen that the two critical points of the fringe pattern are successfully avoided. Figure 4(g) shows the obtained phase result and, for the ease of comparison, the cosine fringe of the obtained phase is shown in Fig. 4(h). The second example is from electronic speckle pattern interferometry with a size of 210×210 and is shown in Fig. 5(a). It has only one critical point but has nonuniform background and modulation, and is also degraded by speckle noise. Figure 5(b) shows the NI map of Fig. 5(a), which well distinguishes the problematical regions in the fringe pattern. Similarly to the first example, four snapshots of the estimated phase of the demodulation of

#165020 - $15.00 USD Received 19 Mar 2012; revised 6 May 2012; accepted 8 May 2012; published 18 May 2012

Fig. 5(a) by the GRPT are shown in Figs. 5(c)-5(f), which clearly indicates that the critical point is successfully postponed to the end of the demodulation. The obtained phase result and its cosine fringe are shown in Fig. 5(g) and Fig. 5(h), respectively. It can be seen that both experimental examples have been satisfactorily demodulated. The calculation time for the GRPT to demodulate Fig. 4(a) and Fig. 5(a) are about 7min and 8min, respectively.

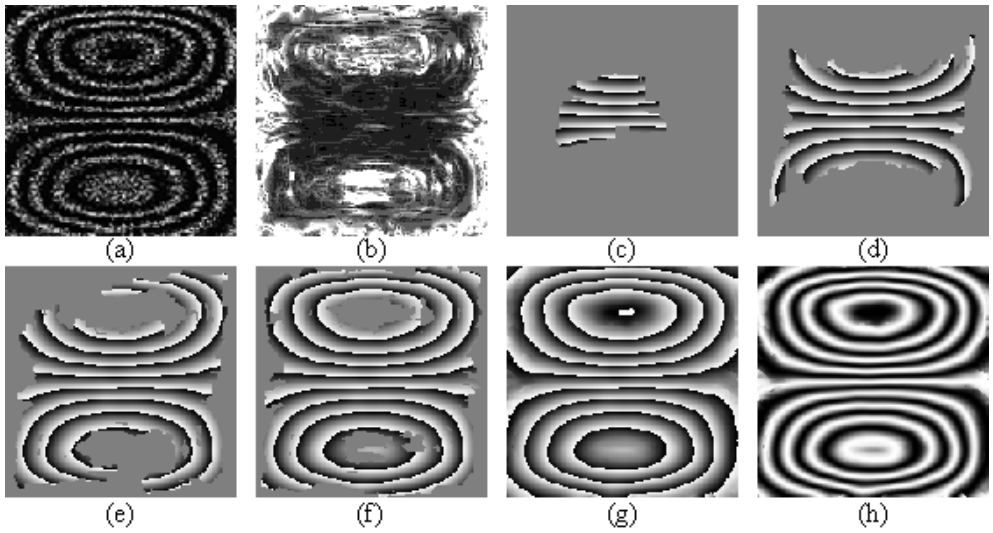

Fig. 4. Experimental fringe pattern demodulated by the GRPT. (a) noisy fringe pattern from speckle shearography; (b) the NI map obtained by the GRPT from the fringe pattern in (a); (c-f) four snapshots of the estimated phase results obtained by the GRPT; (g) rewrapped phase result obtained by the GRPT; (h) cosine value of (g).

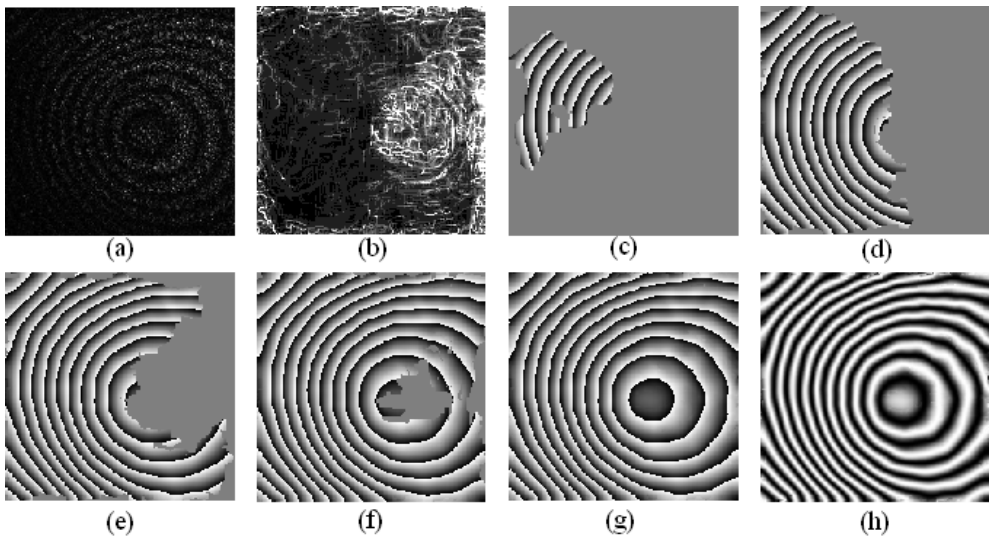

Fig. 5. Experimental fringe pattern demodulated by the GRPT. (a) noisy fringe pattern from electronic speckle pattern interferometry; (b) the NI map obtained by the GRPT from the fringe pattern in (a); (c-f) four snapshots of the estimated phase results obtained by the GRPT; (g) rewrapped phase result obtained by the GRPT; (h) cosine value of (g).

#165020 - $15.00 USD Received 19 Mar 2012; revised 6 May 2012; accepted 8 May 2012; published 18 May 2012

5. Phase demodulation from a single fringe pattern with phase discontinuities by the GRPT

It is of interest to demodulate a single fringe pattern with phase discontinuities. Figure 6(a) shows a simulated example of this issue. It can be seen that the fringe pattern contains three different regions. Each region has its own phase distribution and consequently, the phase distributions at the boundaries of these three regions are discontinuous. The most difficult task for demodulation of such fringe pattern is how to distinguish the different regions and demodulate them separately. The NI guided scanning strategy used in the GRPT provides a possible way to solving this problem, since the NIs at the boundaries are usually large. Figure 6(b) shows the NI map obtained along with the demodulation of Fig. 6(a) by the GRPT, using the same parameters as for Fig. 1. It can be seen that the discontinuous boundaries are clearly distinguished by the large NIs. Figures 6(c)-6(d) show two snapshots of the demodulation of Fig. 6(a) by the GRPT. It can be seen that the discontinuous boundaries are automatically avoided and the different regions are separately demodulated. Figure 6(e) shows the obtained phase result, which is successful and satisfactory. To further verify the effectiveness of the GRPT, Fig. 6(f) shows a noisy fringe pattern with the same phase distribution as Fig. 6(a). Figure 6(g) shows the NI map of Fig. 6(f) obtained along with the demodulation of Fig. 6(f) by the GRPT, using the same parameters as for Fig. 1. Figure 6(h) shows the obtained phase result, which is satisfactory.

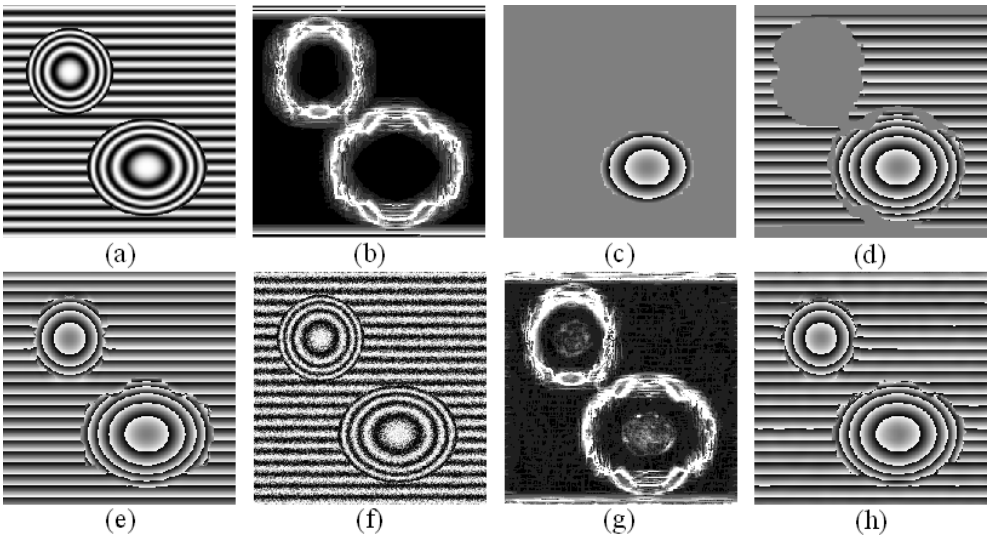

Fig. 6. Fringe pattern with phase discontinuities demodulated by the GRPT. (a) fringe pattern with phase discontinuities; (b) the NI map obtained by the GRPT from the fringe pattern in (a); (c-d) two snapshots of the estimated phase results obtained by the GRPT from the fringe pattern in (a); (e) rewrapped phase result obtained by the GRPT from the fringe pattern in (a); (f) a noisy fringe pattern with the same phase distribution as the fringe pattern in (a); (g) the NI map obtained by the GRPT from the fringe pattern in (f); (h) rewrapped phase result obtained by the GRPT from the fringe pattern in (f).

6. Conclusion

To overcome the two disadvantages of the regularized phase tracker (RPT), i.e., the necessity of a normalized fringe pattern as input and the sensitivity to critical points, a generalized regularized phase tracker (GRPT) is presented with two novel improvements. First, an enhanced cost function is proposed, which uses a general local fringe model that includes a linear background, a linear modulation and a quadratic phase. Second, the number of iterations in the optimization process is used to guide the demodulation path. Based on these two improvements, the GRPT can directly demodulate a single fringe pattern without any pre-

#165020 - $15.00 USD Received 19 Mar 2012; revised 6 May 2012; accepted 8 May 2012; published 18 May 2012

processing and post-processing and successfully solve the problem of the sensitivity to critical points. The GRPT is also shown to be useful to demodulate a fringe pattern with phase discontinuities. Simulation and experimental results are presented to demonstrate the effectiveness and robustness of the GRPT.

Acknowledgments

This work was partially supported by the Singapore MOE Academic Research Fund Tier 1 (RG11/10) and the National Natural Science Foundation of China (NSFC) (No.10902066).

#165020 - $15.00 USD Received 19 Mar 2012; revised 6 May 2012; accepted 8 May 2012; published 18 May 2012